X2B Wide-Angle Steering Mirror

Miroslaw Ostaszewski*, Tim Quakenbush*, Alix Carson* and Jamin Hershberger*

Abstract

Ball Aerospace developed the Wide-Angle Steering Mirror model X2B-WASM with aggressive performance capability and lower cost value. The design of X2B-WASM will be presented along with lessons learned throughout the manufacturing, assembly, integration, and test of this miniaturized fast steering mirror. Engineering/Breadboard/Development testing was completed to verify key performance parameters: ±3 deg of rotation in two axes, greater than 1.0 kHz closed loop bandwidth, and jitter less than 2 μrad.

Overview

The mechanism is comprised of a 26 mm (1.02 in) x 26 mm (1.02 in) mirror that mounts to a Cross Flexure (US Patent US10598924B2) suspension that can achieve ±3 deg of rotation in two axes. Figure 1 shows the CAD model of the X2B-WASM identifying major components: moving mirror assembly with Voice Coil Actuator (VCA) magnets, VCA coils, and proximity position sensor heads mounted to the base assembly.

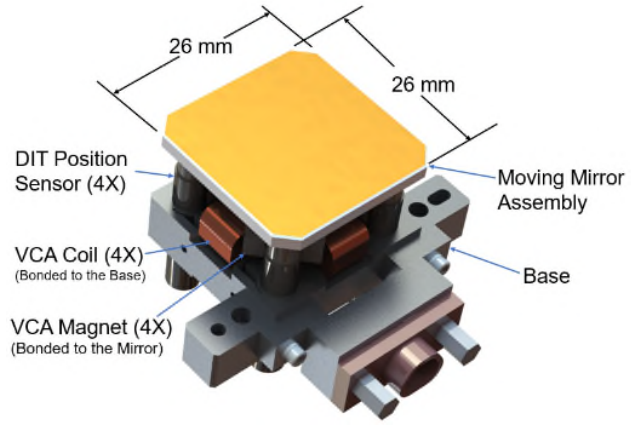

Figure 1. X2B-WASM CAD Model

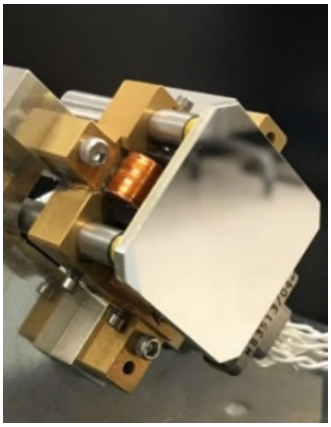

Figure 2. Completed X2B-WASM

The Mirror Moving Assembly tip-tilt motion is driven by a VCA assembly as shown in Figure 3. Four magnets are bonded to the underside of the mirror configured in a magnetic loop with the polarity of magnets as shown. Four coils are bonded to the stationary base and placed in the gaps between magnets. Lorentz force is generated at each coil location with two coil pairs acting in push-pull fashion to produce torque on the moving assembly. The four-coil actuator configuration allows large angular motion within the small volume constraint of the mechanism.

The tip-tilt angle position of the mirror is sensed by a Differential Impedance Transducer (DITs) system. Each DIT sensor head has electrical impedance from the interaction of itself and eddy current in the mirror substrate. The impedance is a function of separation between the sensor head and mirror. The DIT electronics subtracts, demodulates, and amplifies the signals from each pair of sensor heads that are mounted across the center of mirror rotation to give an output signal proportional to mirror angle. DITs angle sensors are common for this type of application and available from several suppliers.

* Ball Aerospace & Technologies Corp., Boulder, CO

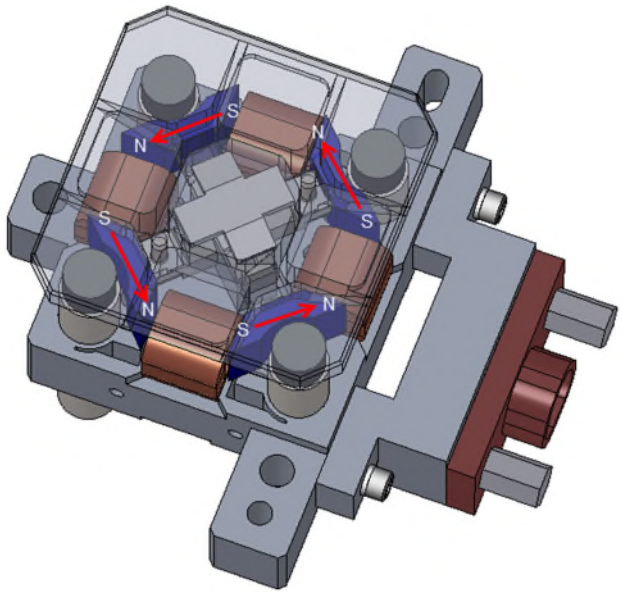

Figure 3. X2B-WASM Magnetic Loop VCA Configuration

Figure 4 shows the two-axis, tip-tilt titanium monolithic flexure; the thin blades in X configuration allow rotation in each axis while being rigid in all translations. The flexure is mounted to a rigid base structure with two 00-90 fasteners and a pin interface that provides precise flexure location on the base. The flexure interface to the mirror with two 00-90 fasteners with mounting locations as shown. Figure 5 shows the small size of the flexure as compared to a penny.

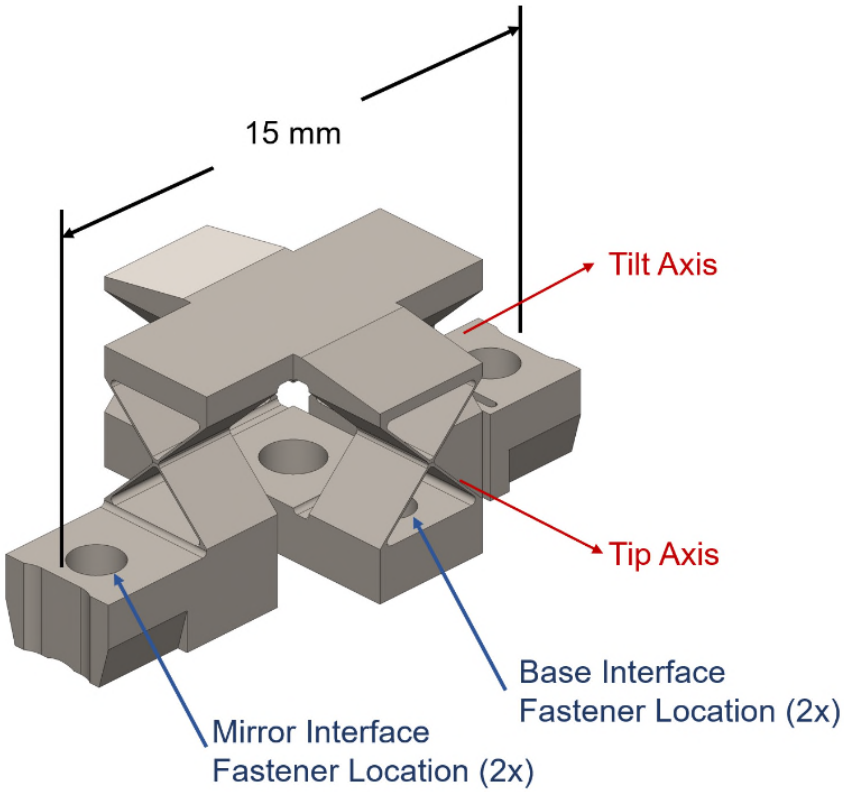

Figure 4. X2B Cross Flexure CAD Model

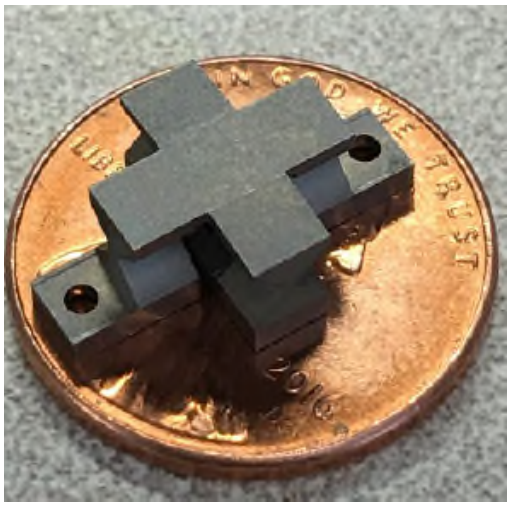

Figure 5. X2B Cross Flexure on a Penny

Table 1. X2B-WASM Performance

Property	Performance
Maximum Range of Travel (Tip, Tilt)	± 3 deg
Residual Mirror Jitter	1.0 µrad RMS
Closed Loop Bandwidth (CLBW) (-3dB)	≥ 1.0 kHz
Mirror Clear Aperture	20.1 mm (0.791 in)
Mirror Surface Figure Error (RMS)	< 23 nm
Rotation Center to Mirror Surface	≤ 4.65 mm (0.183 in)
Total Mass (Mechanism)	Less than 48 gm.
Motor Power at Max Mirror Angle	≤ 2 watts
Launch Load (Static)	100 G axial, 75 G lateral
Launch Loads (Random Vibration)	21.1 G (RMS) overall axial 14.9 G (RMS) overall lateral
Launch Load (Shock)	672 G

Table 2 is a list of measured values for built X2B-WASM units that are referenced throughout this document. Serial numbers that end with the letter “a” indicate values in that row were measured before the unit’s flexure was replaced and “b” designates measurements after flexure replacement. Serial numbers with no letter suffix did not have the flexure replaced. The table is sorted by date to support the flexure design and manufacturing changes that will be described.

Assembly Integration and Test

Maintaining manufacturability of the compact X2B-WASM while ensuring performance metrics were met presented several challenges that required design updates and tooling changes. The serial numbers X2WM1001 - X2WM1005 were built with components using typical tolerances between 0.05 mm (0.002 in) and 0.13 mm (0.005 in). Difficulties during procurement, assembly, integration, and test, led the team to reassess the design from both a manufacturability and producibility standpoint.

Table 2. History of flexure blade thickness effect on 1st & 2nd mode and lifetime.

Build Date yyyy-mm	WASM Serial#	1st Mode (Hz)	2nd Mode (Hz)	CLBW (Hz)	Phase Margin (deg)	Notes
2017-07	X2WM1001	80	950	1200	42	Prototype
2018-07	X2WM1002	18	1110	940	46	Flexure failed in 2020-03 and scrapped.
2020-03	X2WM1003a	16	3500	1180	38	Flexure failed in 2020-12
2020-03	X2WM1004a	18	460	1240	37	Flexure failed in 2020-12
2020-03	X2WM1005a	9 (X) 20 (Y)	560	530	38	Flexure crack suspected
2021-05	X2WM1004b	9	720	1030	40	Updated flexure not available
2021-05	Updated flexures received					
2021-05	X2WM1006	51	1320	590	44	CLBW per system requirements
2021-08	X2WM1003b	43	3500	1030	38	Installed updated flexure
2021-11	X2WM1005b	48	1340	500	39	Installed updated flexure. CLBW per system requirements.

The initial X2B drawings, used for X2WM1001 - X2WM1005, focused on maintaining mirror alignment and optimizing the magnet – coil gap to achieve high motor efficiency across the full range of motion. Actuator performance studies were run on the operational range of travel of the VCAs but did not consider the effect of tolerance stack up. The assembly process relied on complex tooling that proved to be impractical for bond control and produced inconsistency in gap size. For serial numbers X2WM1002a - X2WM1005a the magnet – coil gap resulted in contact between the adjacent magnets and coils. This limited the mechanism range of travel as a magnet face would contact a VCA coil before reaching the hard stop. Additionally, the contact threatened to scratch insulation from coil wires (see Figure 6).

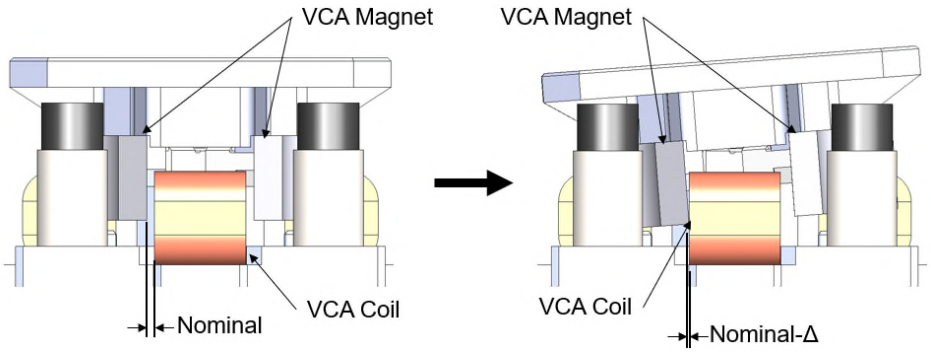

Figure 6. Actuator Gap Across Range of Motion

To investigate the required motor gap to meet performance, a parametric study was devised to analyze the actuator orientation in operation, distances from magnets to VCA coils, and the resultant implied moment on the system. Figure 7 shows the impact of the actuator gap on VCA performance. The nominal gap of 0.51 mm (0.02 in) shows peak performance with larger gaps showing degradation in performance.

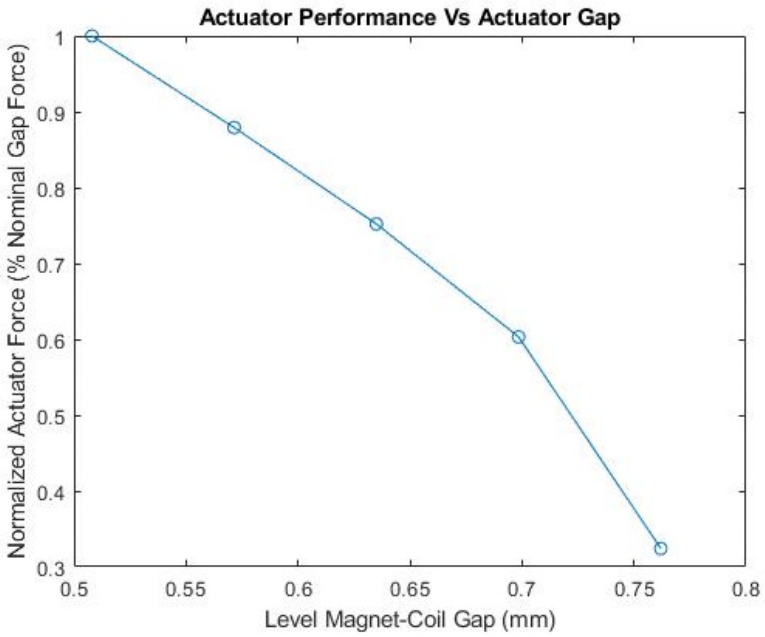

Figure 7. Actuator force vs. magnet-coil gap (mm)

A study of mirror motion found that the assembly required a minimum of 0.33 mm (0.013 in) of clearance between the coils and the magnets at the 0 deg tip and tilt position to allow for full rotation of the mirror. In addition, it was found the assembly could tolerate up to 0.64 mm (0.025 in) of VCA gap before VCA performance degraded to 75% of nominal. A nominal designed gap of 0.51 mm (0.020 in) was selected.

The design was revaluated through a tolerance analysis to assess how the required magnet – coil gap should be controlled. The mechanism is broken into two modular sub-assemblies: the Baseplate Assembly (BA) consisting of the Baseplate, VCA coils and DITs, and moving mirror assembly (MMA) consisting of the Mirror, Flexure and VCA magnets. The interface between these two sub-assemblies consists of a locating emboss and two screws. It was determined that if both the pattern of mirror magnets on the MMA and pattern of VCA coils on the BA were controlled during assembly, then the interface between the MMA and BA could be adjusted at final assembly to achieve the correct VCA gap size. The pattern of VCA coils is controlled by tight position tolerances on the pattern of slots the coils are bonded to in the baseplate. The mirror magnet pattern is controlled via bond tooling, which allows for the pattern to be measured and adjusted prior to bonding. At final assembly, the MMA can be adjusted rotationally relative to the BA until the desired gap size is achieved for all VCA gaps in the system. This is accomplished with simple go/no-go shim stock.

To improve tooling, a cross functional collaboration took place between engineers and technicians to validate a new procedure. Rapid prototyping was used to print mock-ups of new tooling designs, as well as an actual mechanism assembly. This allowed for quick feedback and design iteration to finalize new tooling and assembly procedures that met cost, reduced in touch-labor time, and increased repeatability for gap control.

Figure 8 shows one iteration of the magnet bonding tooling. Note the shims used to set each magnet gap. It is important to state that the magnets have a strong attraction. During the first brass board unit builds, it was observed that magnets shifted during the bond cure. To reduce this behavior, magnets are bonded sequentially and then secured in place by setscrews to restrict movement during cure. Figure 8 shows the final magnet bonding tooling and the magnets being secured in place by nylon tip set screws.

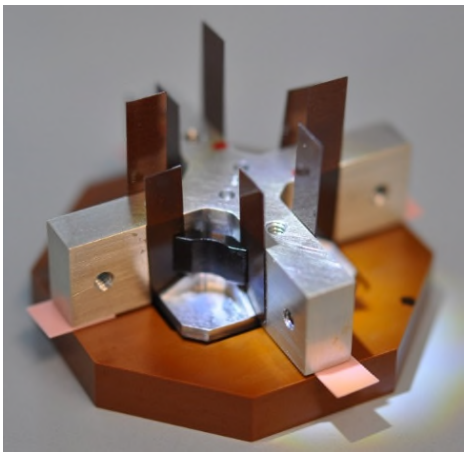

Figure 8. Magnet Bond Tooling

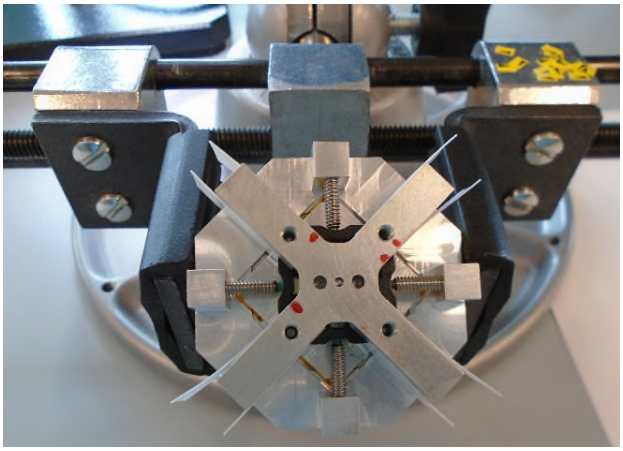

Figure 9. Magnet Bond during Cure

The initial X2B-WASMs also exhibited extremely fragile flexures with cross blades approximately one-third the thickness of a sheet of printer paper, 0.0381-mm (0.0015-in) thick. To assemble the flexure onto the mirror substrate, two fasteners are tightened in an alternating pattern, see Figure 10. Due to the flexure's susceptibility to damage, it is important to ensure that the flexure mounting pads are flat against the mirror substrate mounting pads before torquing the fasteners. There is limited visibility to confirm the flexure position after torquing the fasteners.

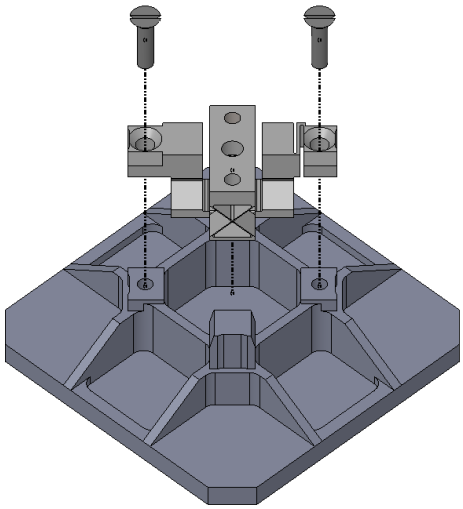

Figure 10. Mirror Substrate and Flexure Subassembly

If the flexure is not mounted with its pads flush to the mirror pads, the flexure is at an increased risk of breaking at the higher assembly. The MMA is pulled onto the baseplate assembly using two fasteners that thread onto the flexure through the baseplate, see Figure 11. Again, this operation has no visibility of the flexure to confirm the condition of the cross blades after assembly. It is during this assembly that a misaligned flexure's cross blades are at a greater risk of yielding due to the tension from threading a fastener into the flexure. The risk of flexure failure during assembly led to a design analysis of the flexure blade thickness to attempt to increase the structural integrity of the design.

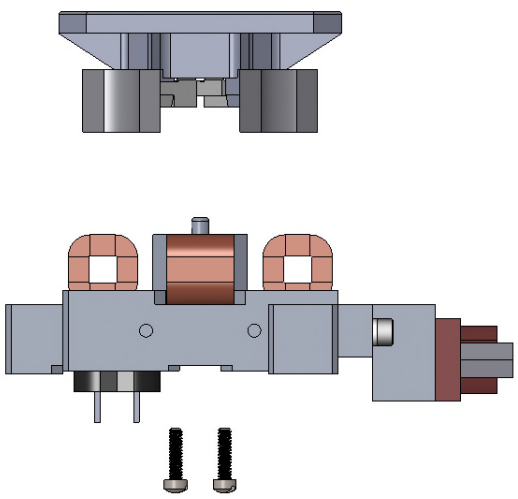

Figure 11. Moving Mirror Subassembly and Baseplate Assembly Integration

Due to the packaging constraints, 00-90 fasteners are necessary to attach the flexure to both the mirror and baseplate. The 00-90 fasteners represent a hurdle for procurement as they are non-standard fastener per ASME B18.3. Certified supply for these fasteners is not reliable. During assembly of serial numbers X2WM1002a - X2WM1005a, the original supplier discontinued their production of these fasteners. An order for certified 00-90 fasteners was placed with a new supplier for future flight builds. The brass board development units were completed with non-flight 00-90 fasteners that could be procured quickly and met the needs of the brass board test plan. These types of substitutions may not be palatable for flight programs. For future flight builds, ample procurement time is necessary to ensure the availability of flight rated hardware.

Flexure Design and Analysis

The titanium (TI-10V-2FE-3AL) cross flexure fits in a 15.2 mm (.598 in) X 88.9 mm (3.5 in) X 5.46 mm (.215 in) volume. The key parameters considered for the flexure design were first mode frequency of the MMA and the mechanism power consumption. The desired first mode frequency is 40-50Hz to achieve the 1-kHz bandwidth and the max angle power budget of 2 W. The flexure is manufactured by Electrical Discharge Machining (EDM) processing, followed by an etch bath for recast removal. To validate the process, the supplier provides a coupon that is used to examine surface finish, recast removal, and final cross blade thickness. The recommended minimum tolerance for wire EDM and recast removal is .005 mm (.0002 in).

The first mode frequency and power consumption of the mechanism are driven by the thickness of the cross blades. A thicker cross blade increases the blade stiffness, increasing the first mode frequency and power needed to hold the mirror at the maximum angle of travel. The initial design set the flexure blade thickness to 0.0483 mm (.0019 in) ± 0.0025mm (.0001 in), a thickness that proved to have reliability and manufacturability concerns. The design pushed beyond the limit of repeatable wire EDM and etching capabilities, and three flexures built in the first lot ended up being only 0.0381-mm (.0015-in) thick. With blades that thin, the mechanism assembly was unstable during calibration and vulnerable to damage during assembly and test. Once assembled, visual inspection is not possible to identify a damaged flexure; failure is identified during X2B-WASM calibration and testing. A damaged flexure often presents a lower first mode frequency, shifted mode frequencies at larger angles of travel, or a null pointing position offset at calibration.

Lab vibration testing was performed on two of the units. The mirror-flexure subassemblies sheared off the baseplate. The post-mortem inspection started the effort to enhance the design to improve reliability,

manufacturability, and minimize risk. It is believed that the flexures were damaged during assembly and buckled during testing.

The second-generation cross flexure aimed to improve the design by analyzing the optimal blade thickness to maintain the desired first mode frequency, meet power requirements and survive assembly, integration, and test. To find the optimal blade thickness to meet frequency and power requirements, a program was developed in MATLAB to relate first mode frequency and power consumption. To predict first mode frequency for a given blade thickness, a structural analysis was completed to determine an approximate first mode. The flexure blade thicknesses of 0.0381 mm (0.0015 in), 0.0483 mm (0.0023 in), 0.0635 mm (0.0025 in), and 0.0686 mm (0.0027 in), were selected for analysis. Figure 12 plots a linear curve fit of the predicted first mode frequency against flexure blade thicknesses.

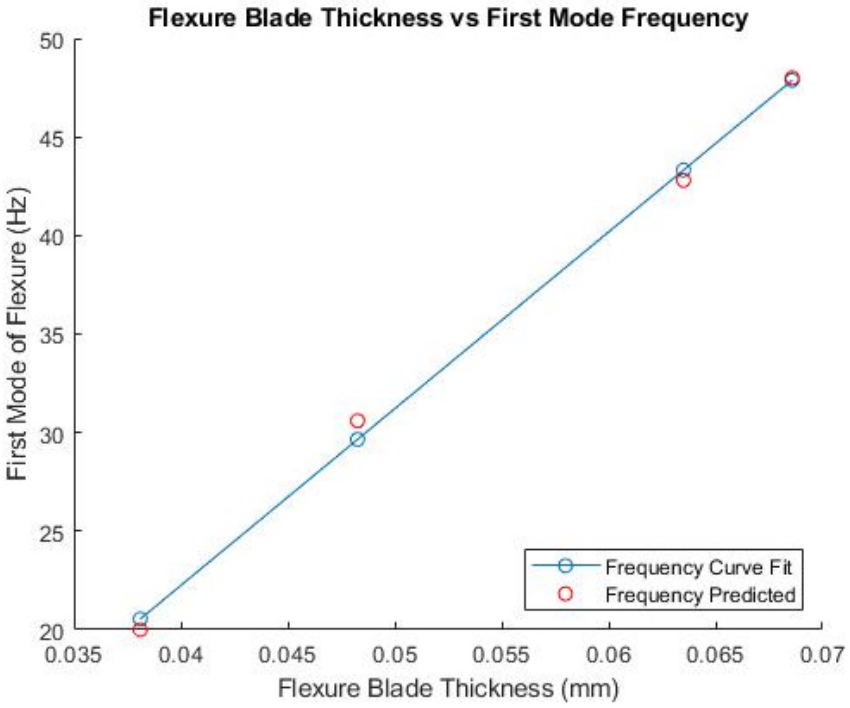

Figure 12. Flexure Blade Thickness (mm) vs First Mode Frequency (Hz)

To predict power consumption for a given blade thickness, the power consumed by the X2B-WASM serial numbers X2WM1003a, X2WM1004a, and X2WM1005a from Table 2 were interpolated to create a polynomial curve fit that could predict power consumed for a given blade thickness. To find the predicted power for the analyzed blade thicknesses, the first mode frequencies determined from the structural analysis are used to find the spring rate, and therefore holding current, needed to maintain the maximum angle of travel. The power is then calculated by multiplying the square of the holding current by the resistance of the four coils. Figure 13 plots the predicted first mode frequency against the predicted power needed for maximum angular travel for the selected flexure blade thicknesses. After running the MATLAB program, the flexure blade thickness 0.0635 mm (0.0025 in) had a predicted first mode frequency of 42.8 Hz and a max angle power consumption of 2.07W. This met the target for those two parameters. The predicted values can be compared to the actual measurements provided for X2WM1003b defined by Table 2 and Figure 17 for a percent error of roughly 12% for the first mode frequency and 18% for the power budget. Given the small sample size for analysis, it is not unexpected to have a percent error greater than 10%.

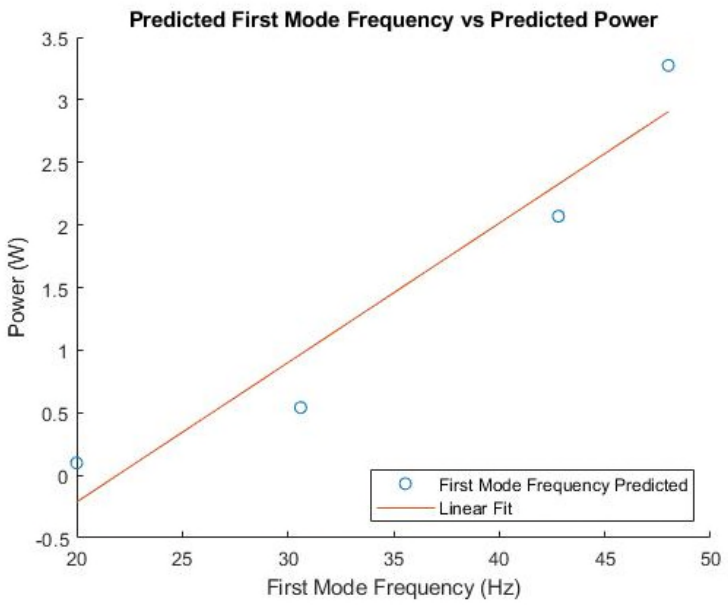

Figure 13. First Mode Frequency (Hz) vs Predicted Power (W)

After down selecting to the 0.0635-mm (0.0025-in) blade thickness, the performance for the 0.0635-mm (0.0025-in) and 0.0381-mm (0.015-in) flexures were evaluated in a simulated vibration environment. The flexures were analyzed at a random vibration of 0.44 g^2/Hz, shock at 672 G, and tilt of 3 deg to determine maximum stress along the flexure axis. Table 3 compares the analyzed stress on the flexures under the defined environments. It is expected to see a higher stress for the thicker flexure due to mirror tilt as the thicker flexure will be stiffer, making the blade less compliant to bending.

Table 3. Structural Analysis Margin of Safety Parameters

Flexure	Max Stress due to 1G Shock (along flexure axis)	Max Stress due to Random Vibe (All Axis)	Max Stress Due to Mirror Tilt (3 deg)
.0381 mm (.0015 in)	3.3 MPa (0.48 ksi)	141 MPa (20.5 ksi)	119 MPa (17.2 ksi)
.0635 mm (.0025 in)	2 MPa (0.29 ksi)	140 MPa (20.3 ksi)	197 MPa (28.6 ksi)

The analysis predicted the 0.063-mm (0.0025-in) thick flexure blade to have improved stress for random vibration and shock with buckling at 0.29 G^2/Hz (see Figure 14), which met the outlined mechanism performance. This flexure blade thickness also met the target first mode frequency and max angle power budget.

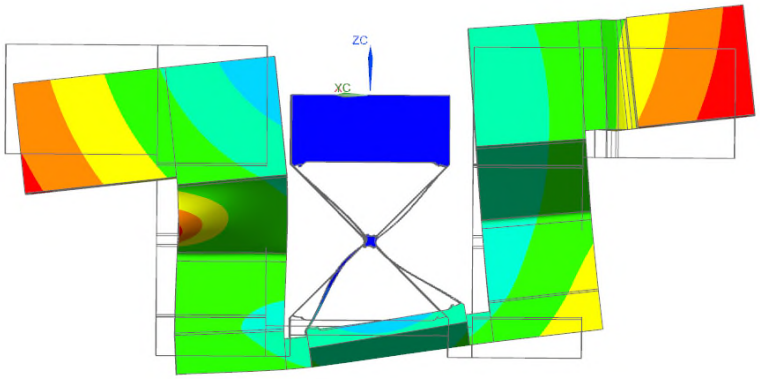

Figure 14. Flexure Blades Begin to Buckle at 0.29 G^2/Hz

Measured Performance

The X2B-WASM is designed to exceed 1-kHz bandwidth with good stability margins. The batch of flexures with blades made too thin had reduced performance because of vibration modes that change with mirror angle (see WASM serial numbers 1002, 1003a, 1004a and 1005a in Table 2). As each flexure failed during lab testing, they were replaced with correctly manufactured flexures (see WASMs with build dates after May 2021 in Table 2). The exception is serial number X2WM1001, which has the first prototype flexure that is slightly different than all the other steering mirrors in the table.

A primary limitation to closed loop bandwidth is the second vibration mode type and frequency. If the vibration mode is mechanically between the motors and sensors, the plant transfer function phase shift will be negative and is more likely to cause stability problems. If that mode frequency is too close to the desired open loop crossover, notch filters will not help, and the crossover (and bandwidth) will need to be reduced.

The X2B-WASM second vibration mode is more forgiving. The phase bump is very small, moves in a positive direction, and has frequency much higher than the open loop crossover (see 1200-Hz mode in bottom of Figure 15). The magnitude and frequency also have minimal change over mirror angle range. This means the high bandwidth (1030 Hz in Figure 15) is achievable without additional notch or low pass filters. Small signal bandwidth higher than 1200 Hz is possible by designing electronics and compensator to reduce the phase loss at frequencies above 1000 Hz, using a flexure with higher first mode frequency, and incorporating possible notch filters to attenuate and problematic vibration modes.

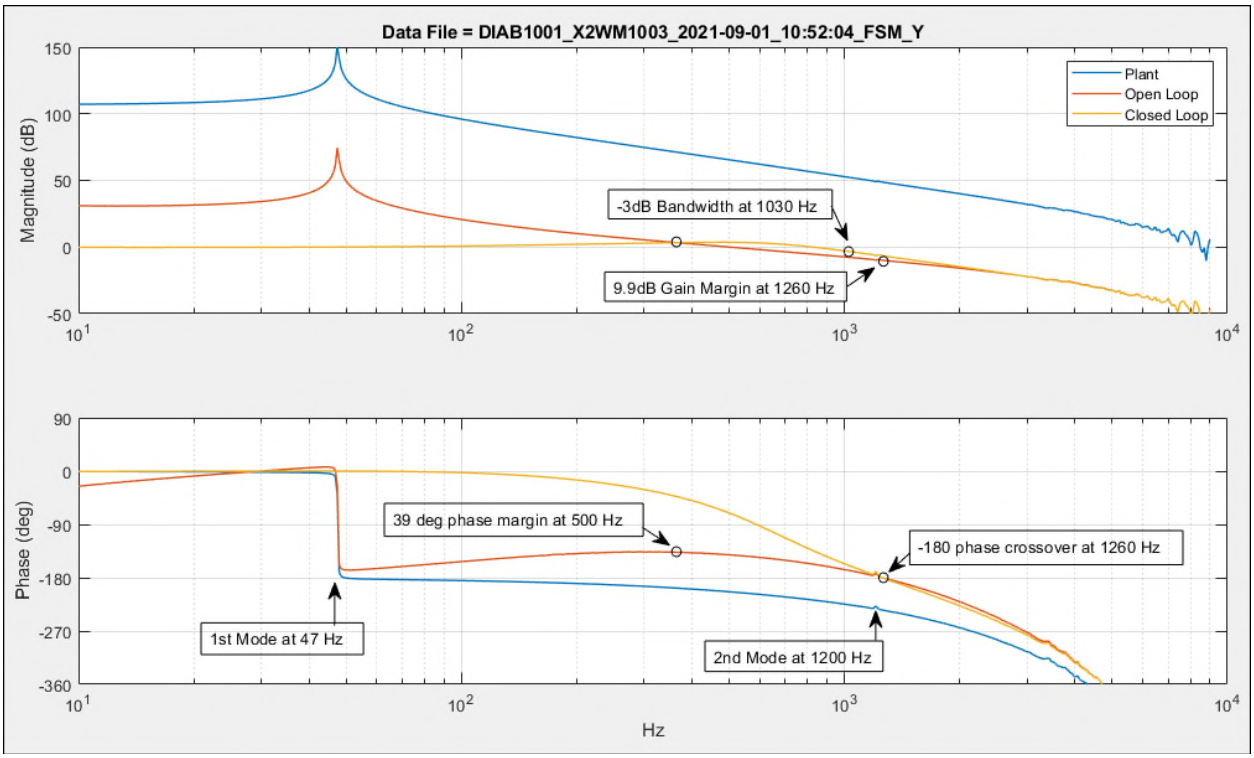

Figure 15. Transfer functions of X2WM1003 with updated flexure design

Figure 16 shows the measured estimate for residual jitter is 1 µrad RMS for serial number X2WM1003b. The jitter estimate starts with blocks of time series data that were recorded at 49 different mirror positions across the range of travel. The sample rate, and compensator update rate, was 20 kHz. A power spectral density (PSD) curve was calculated from each time series block. The top graph in Figure 16 is the mean of all the PSD curves and the bottom graph is the forward RMS sum curve. The forward sum at 10 kHz in Figure 16 is 1.8 µrad RMS and the largest of the 49 forward sum curves is 2.05 µrad RMS.

Previous comparison of steering mirror position data with mirror angle measured with a 3-axis interferometer revealed that mirror residual jitter can be approximated by integrating the PSD curve up to the mechanism closed loop bandwidth. That point is indicated by a red circle in the bottom curve of Figure 16 with coordinate values 1030 Hz and 1.0 µrad RMS.

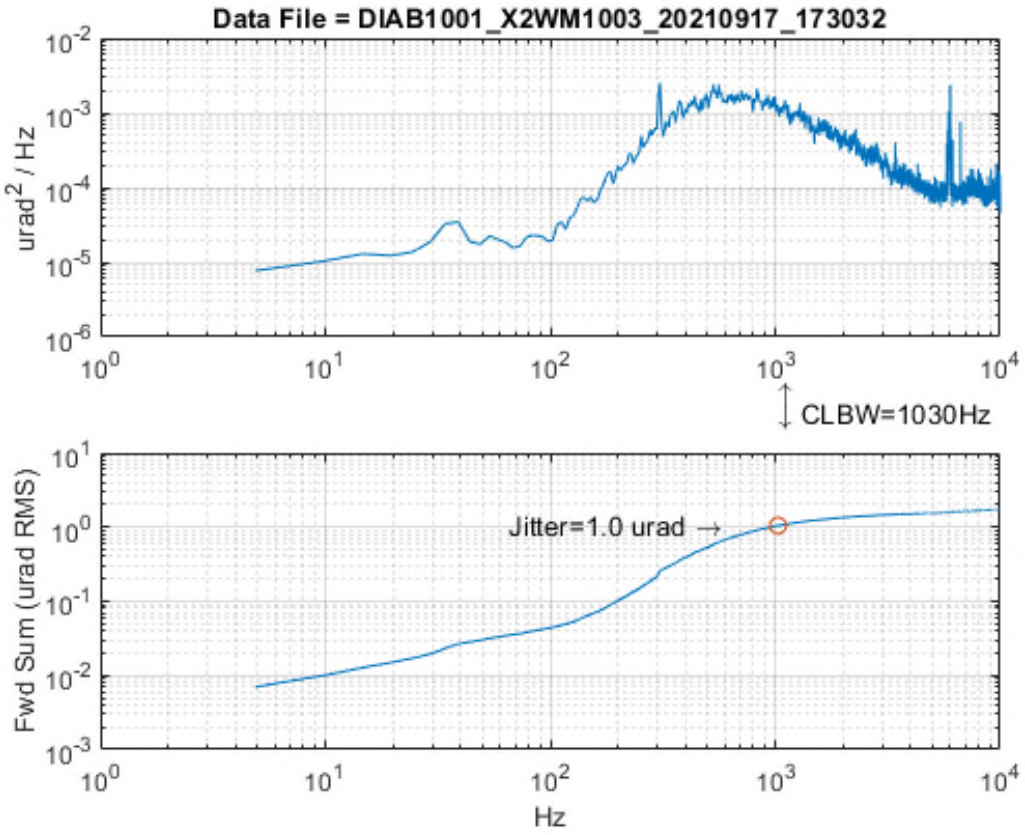

Figure 16. PSD curve (top graph) and forward RMS sum of mirror angle signal (bottom graph)

Figure 17 is a graph of motor power calculated from motor resistance and motor current data recorded during angle calibration of serial number X2WM1003b. This reflects the power to hold against the flexure spring constant. Mechanism power will be larger when rejecting base motion disturbance and performing continuous scan profiles.

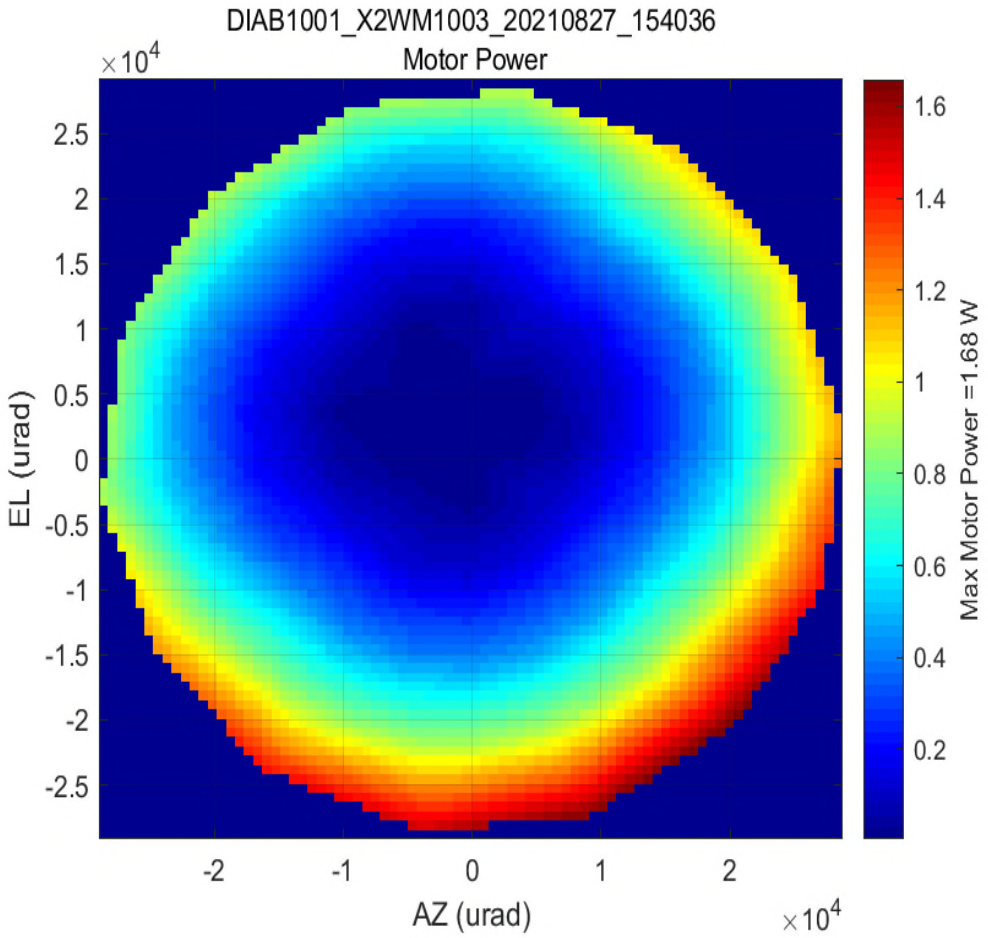

Figure 17. Motor power vs. angle for X2WM1003b

Conclusion

The compact Wide Angle Steering Mirror, X2B-WASM development presented many challenges during assembly, integration, and test. Assembly of the small mechanism required thoughtful tooling design to ease assembly, improve alignment, and maintain performance. In designing a miniature mechanism, one key takeaway is to focus on modularity of the system. Modularity allowed there to be more visibility during assembly of each piece part which led to simplified assembly processes, lower risk of piece part damage, and reduction of in-touch labor. Additionally, one must identify the gating manufacturing processes early in the design phase. The ideal design for performance may never be achievable due to manufacturing limitations. Failure of the key component, the two-axis cross flexure, due to manufacturability, required detailed analysis and test to converge on an optimal solution. Testing of the optimized development unit showed the mechanism capable of ±3 deg of rotation travel in two axes with 1.0-kHz closed loop bandwidth and residual jitter under 2 µrad RMS. The redesign efforts of the X2B-WASM resulted in a robust design that meets the desired performance parameters.